

# KINETIC STUDIES FOR GOLD LEACHING OF A REFRACTORY SULFIDE CONCENTRATE BY CHLORIDE–HYPOCHLORITE SOLUTION

M. Ghobeiti Hasab, F. Rashchi\* and Sh. Raygan

\* rashchi@ut.ac.ir

Received: November 2013

Accepted: January 2014

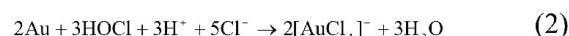
School of Metallurgy and Materials Engineering, College of Engineering, University of Tehran, Tehran, Iran.

**Abstract:** In this paper, gold leaching of a refractory sulfide concentrate by chloride–hypochlorite solution was investigated and effects of stirring speed, temperature and particle size on the leaching rate were reported. Experimental data for leaching rate of gold were analyzed with the shrinking–core model. Results were consistent with chemical reaction control mechanism in the first 1 h of leaching and diffusion control mechanism in the second 1 h. Apparent activation energy also was found to be 22.68 kJ/mol in the first step and 3.93 kJ/mol in the second step of leaching.

**Keywords:** Gold concentrate, Non–cyanide leaching, Chloride–hypochlorite, Kinetic.

## 1. INTRODUCTION

Hypochlorite solution has been recognized as a strong oxidizing reagent to oxidise metal sulfides to sulfates and metal ions even at room temperature [1, 2]. In this solution, depending on pH, various species of hypochlorite ion ( $\text{OCl}^-$ ), hypochlorous acid ( $\text{HOCl}$ ) and aqueous chlorine ( $\text{Cl}_2$  (aq)) are produced. Hypochlorite ion predominates at high pH values. Hypochlorous acid becomes predominant at pH values below 7.5. At low pH values ( $< 3.5$ ), aqueous chlorine predominates and if its concentration in solution is more than the solubility of chlorine in solution, chlorine gas can be evolved from the solution. Among these species, hypochlorous acid is the most effective oxidant [3]. This oxidant is suitable for leaching of gold as  $[\text{AuCl}_4]^-$  complex in chloride media. At a solution with ca. 2 M chloride and potentials greater than 900 mV (vs. SHE), this complex is stable in the 0–8 pH range [4]. For refractory sulfide gold ores, which gold occurs finely disseminated in the matrices of the base metal sulfide minerals such as iron sulfide, using hypochlorite solution at pH range of hypochlorous acid and in chloride media can simultaneously oxidise metal sulfides and leach gold. Oxidation of iron sulfide and leaching of gold by hypochlorous acid are expressed according to equations (1) and (2) [5].



A few researchers have investigated the leaching of gold from an ore or a concentrate by chloride–hypochlorite solution. Puvvada and Murthy [6] during leaching of gold from a chalcopyrite concentrate reported that the gold dissolution rate is independent of the level of sodium hypochlorite ( $\text{NaOCl}$ ) within the 25–75 g/L range, 25 g/L  $\text{NaCl}$  and 0.35 M  $\text{HCl}$  at solid–liquid ratio of 1:4, leaching time of 4 h and room temperature. The gold recovery only reached 32% at three different levels of  $\text{NaOCl}$ . Increasing the  $\text{NaCl}$  concentration from 25 to 200 g/L resulted in both enhanced reaction rate and gold recovery to a maximum of 45%. Baghalha [7] studied the leaching of gold from an oxide ore. At solid–liquid ratio of 1:3, temperature of 25 °C, stirring speed of 600 rpm, 10 g/L  $\text{OCl}^-$ , 9 g/L  $\text{HCl}$  (initial pH 7.3) and 100 g/L  $\text{NaCl}$ , about 70% of gold was dissolved into solution in 4 h. Soo Nam et al. [8] using sodium hypochlorite solution at pH of 4 (adjusted by  $\text{HCl}$ ) and 3 M  $\text{NaCl}$ , at solid–liquid ratio of 1:1, ambient temperature and stirring speed of 500 rpm, extracted 80% of gold from an oxide tailing sample during 2 h. The solution Eh was adjusted

at about 1000 mV to stabilize gold as soluble form. However, in these researches effect of kinetic parameters have not been considered.

In the leaching processes, effective kinetics parameters on the leaching rate are stirring speed, temperature and particle size as well as concentration of reactants. In this paper, the effects of stirring speed, temperature and particle size on the leaching of a gold-bearing sulfide concentrate by chloride-hypochlorite solution will be investigated.

## 2. EXPERIMENTAL PROCEDURE

### 2.1. Materials Characterization

The concentrate used in this study was obtained by flotation of an ore located in north-western of Iran (Barika Mine in Sardasht). Particle size analysis by particle size analyser (model: CILAS 1064) showed that 90% of particles are finer than 37.4  $\mu\text{m}$ . Phase analysis of concentrate by XRD (model: Philips X'pert, Cu-K $\alpha$  radiation) showed that major phases present are quartz ( $\text{SiO}_2$ ) and pyrite ( $\text{FeS}_2$ ) along with minor phases of barite ( $\text{BaSO}_4$ ) and muscovite ( $\text{H}_2\text{KAl}_3(\text{SiO}_4)_3$ ) (Fig. 1).

Mineralogical studies using thin and polished sections under optical microscopy showed that in

addition to the mentioned minerals, sphalerite ( $\text{ZnS}$ ), calcite ( $\text{CaCO}_3$ ), galena ( $\text{PbS}$ ), pyrrhotite ( $\text{FeS}$ ), chalcopyrite ( $\text{CuFeS}_2$ ), bornite ( $\text{Cu}_5\text{FeS}_4$ ), tetrahedrite ( $(\text{Cu,Fe})_{12}\text{Sb}_4\text{S}_{13}$ ), arsenopyrite ( $\text{FeAsS}$ ) and argentite ( $\text{Ag}_2\text{S}$ ) were also presented at trace values. Gold was found as electrum alloy ( $\text{Au-Ag}$ ) and conflicted with pyrite.

Table 1 shows major elements composition of the concentrate which were analyzed by XRF (model: Philips PW1480), Au was analyzed by the fire assay. As it is shown the concentrate contains 20.45 g/t gold.

### 2.2. Equipments and Procedures

A four-neck pyrex flask equipped with a reflux condenser, a thermometer, a pH meter and an ORP meter (vs. SHE) was used as the batch reactor. The flask was immersed in an aluminum bowl containing water for temperature control with  $\pm 2$   $^\circ\text{C}$  tolerance. Stirring speed and temperature were controlled by a magnetic stirrer equipped with hot plate. To run a leaching experiment, first a leachant solution containing 200 g/L calcium hypochlorite ( $\text{Ca}(\text{OCl})_2$ ) and 100 g/L sodium chloride ( $\text{NaCl}$ ) in deionized water was prepared. All the reagents were analytical grade from Merck. The mentioned amounts which were considered as optimum

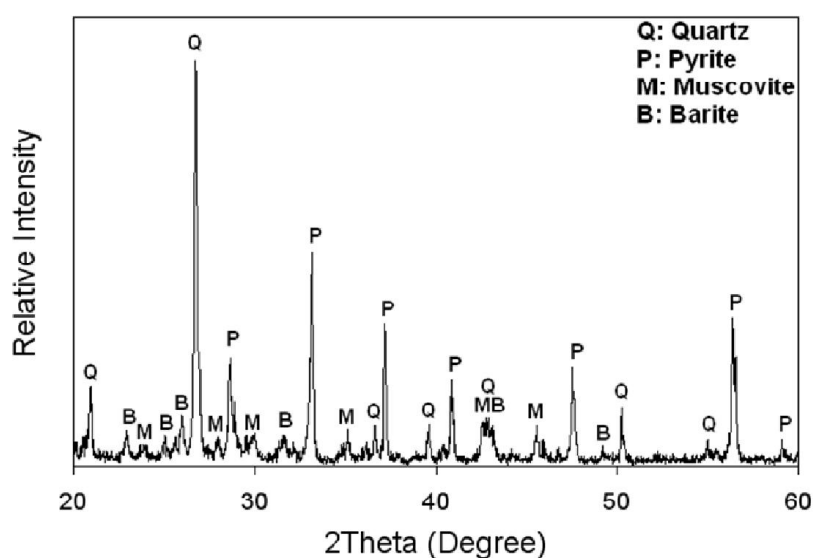


Fig. 1. XRD pattern of the used concentrate.

**Table 1.** Major elements composition of the concentrate (the oxygen content is not included)

Si (%)	S (%)	Fe (%)	Al (%)	K (%)	Ba (%)	Zn (%)	Ca (%)	Pb (%)	Cu (ppm)	Sb (ppm)	As (ppm)	Ag (ppm)	Au (ppb)
17.76	13.68	12.79	5.93	2.26	1.84	1.79	0.75	0.51	3994	1870	1689	1650	20451

concentrations were resulted from an earlier research [9] working on this concentrate. For each experiment, 100 mL of the leachant solution was transferred into the reactor and heated up to reach at required temperature. Thereafter, 20 g concentrate was added to the reactor (solid to liquid ratio (S/L) = 1/5) and the contents were well agitated. Initial stirring speed was selected 600 rpm for a good mixing. The slurry pH and ORP (oxidation–reduction potential) were controlled throughout the process. In all tests, two important conditions were prevented; dropping of pH to below 3.5 (formation of chlorine gas) and dropping of the ORP to less than 900 mV (instability of gold complex). At the defined interval, 5 mL of the slurry was withdrawn using a pipette and filtered by filter paper immediately, then analyzed for gold by ICP (model: VISTA–PRO). The solid residues were rinsed with deionized water and dried at 80 °C for 2 h, then analyzed by SEM (model: TESCAN) equipped with EDX (model: SAMx).

### 3. RESULTS

#### 3.1. Initial Studies

Fig. 2 (a) shows changes of the slurry pH during 3 h (1st stage) of leaching of the concentrate at 600 rpm and 25 °C. the initial pH of the leachant is about 11. As it is shown during the first 1 h, pH drops. Dropping pH is due to oxidation of sulfide and production of acid. After 60 min, pH stayed constant indicating the end of the oxidation of metal sulfides. Small increase in pH during 60 to 180 min may be due to consumption of produced acid in reaction with gangue minerals.

Changes of the slurry ORP during 3 h of leaching (Fig. 3 (a), 1st stage) indicates the ORP corresponding to pH drop, increased. At pH below 7.5 where HOCl is the most oxidant, pH drop occurs sharply (indicating the fast oxidation of metal sulfides) and ORP has the highest value. Decreasing of ORP during 60 to 120 min is probably due to the consumption of oxidant in the oxidation reactions.

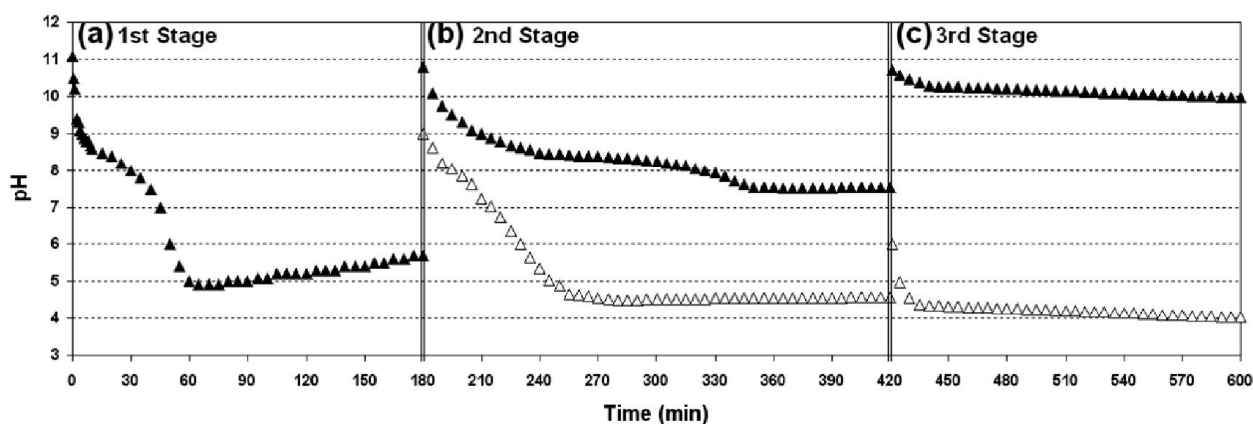


**Fig. 2.** Changes of the slurry pH during leaching of (a) the concentrate (b) the residue of 1st stage washed with HCl (c) residue of 2nd stage washed with HCl (▲: without addition of sulfuric acid, △: with addition of sulfuric acid).

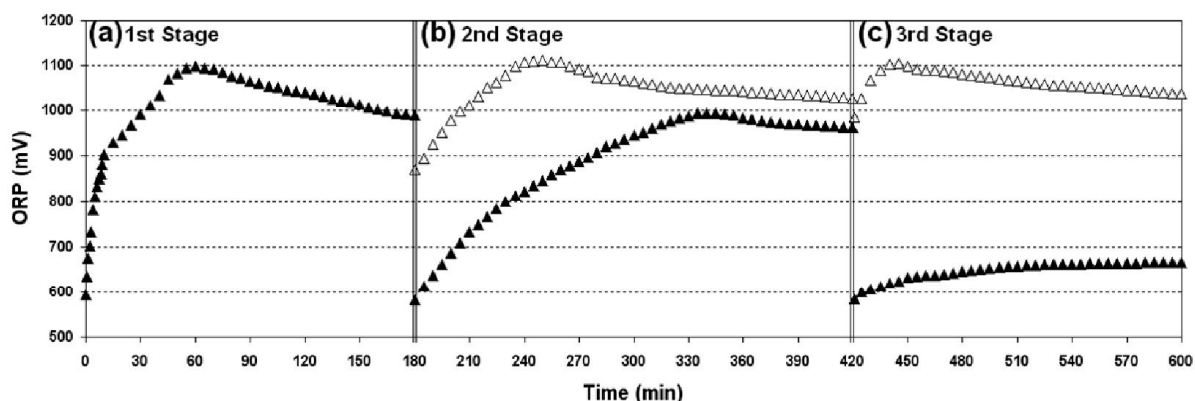


Fig. 3. Changes of the slurry ORP during leaching of (a) the concentrate (b) the residue of 1st stage washed with HCl (c) residue of 2nd stage washed with HCl ( $\blacktriangle$ : without addition of sulfuric acid,  $\triangle$ : with addition of sulfuric acid).

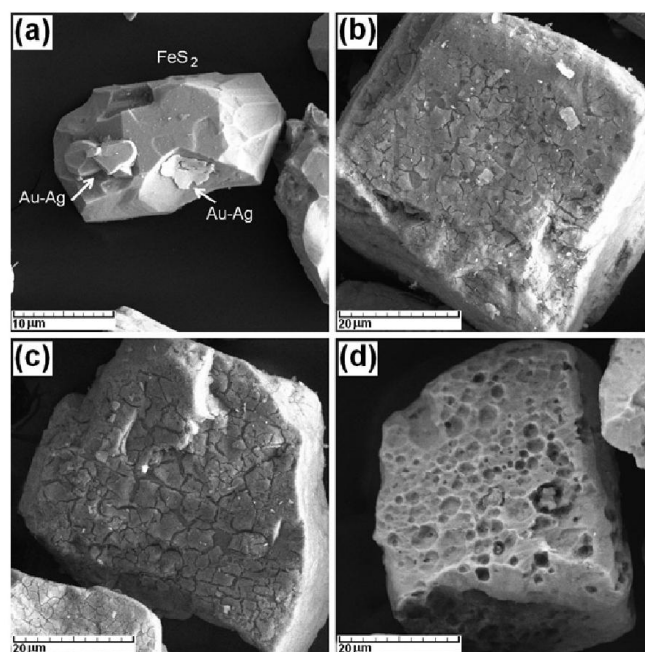


Fig. 4. SEM images of the concentrate (a) before leaching (b) after 1 h leaching (c) after 3 h leaching (d) after 3 h leaching and washed with HCl.

Fig. 4 (a) shows SEM image of a pyrite particle of the concentrate before leaching. Some 5  $\mu\text{m}$  particles of electrum conflicted with pyrite were observed. Figs. 4 (b) and (c) show the residue resulted after 1 and 3 h leaching, respectively. As it is shown during leaching, a layer is formed on the surface from oxidation of pyrite. Point analysis by SEM/EDX characterized this layer as iron hydroxide ( $\text{Fe}(\text{OH})_3$ ) that due to its amorphous structure cannot be identified by

XRD. The residue was washed with hydrochloric acid at  $\text{pH} < 1$  for 15 min ( $S/L=1/2$ ,  $25\text{ }^\circ\text{C}$ , 400 rpm) to remove the layer and filtered; then, it was rinsed with deionized water and dried. Fig. 4 (d) shows a pyrite particle with the removed hydroxide cover. Destructive effect of the oxidant (hypochlorous acid) over the surface of pyrite was clearly observed.

Figs. 5 (a)–(c) show images of the concentrate in polished section after 1 h leaching. It was

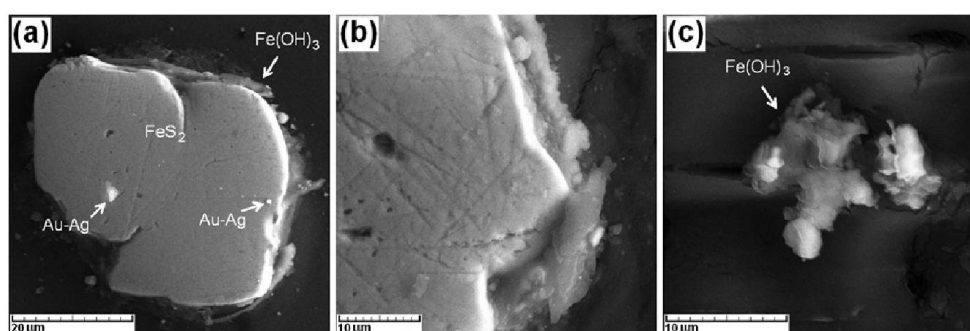


Fig. 5. SEM images of the concentrate after 1 h leaching, in polished section, (a), (b) a large particle of pyrite containing of product layer (c) a small particle of pyrite which has been completely oxidised.

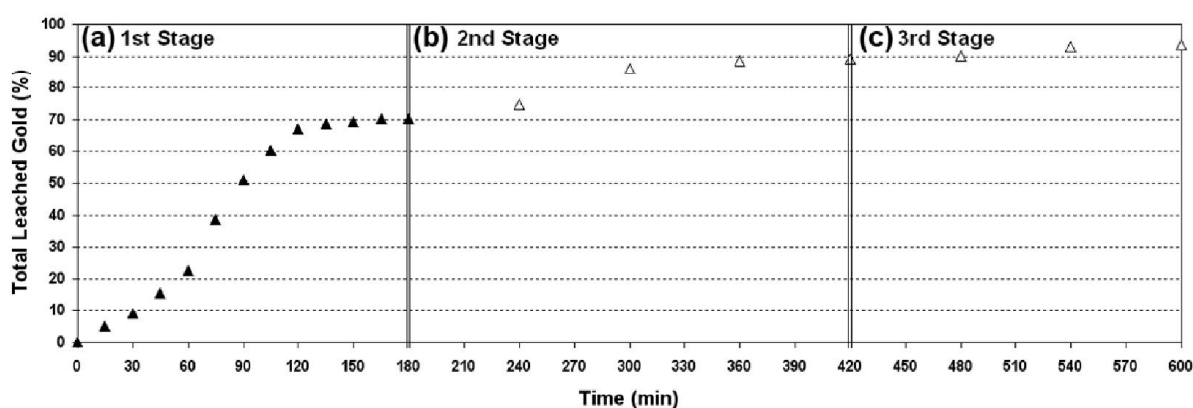


Fig. 6. Total percent leached gold during leaching of (a) the concentrate (b) the residue of 1st stage washed with HCl (c) residue of 2nd stage washed with HCl ( $\blacktriangle$ : without addition of sulfuric acid,  $\triangle$ : with addition of sulfuric acid).

observed that the large particles of pyrite contain a layer (Figs. 5 (a) and (b)), while the particles finer than 10  $\mu\text{m}$  have been oxidised completely (Fig. 5 (c)). The thickness of the passive layer is thinner than 5  $\mu\text{m}$ . This layer prevents the pyrite oxidation, since the oxidant cannot diffuse through the coating to reach the pyrite surface [10].

The residue washed with hydrochloric acid was leached again at solution containing 100 g/L  $\text{Ca}(\text{OCl})_2$  and 100 g/L NaCl for 4 h (S/L=1/5, 25°C, 600 rpm). Figs. 2 (b) and 3 (b) with black symbols ( $\blacktriangle$ ) show the changes of the slurry pH and ORP during leaching, respectively. To improve the pH and ORP condition of leaching, initial pH was adjusted to 9 by adding sulfuric acid which in this case changes of pH and ORP were remarked by white symbols ( $\triangle$ ) in Figs 2(b) and 3 (b). Again residue of this stage (2nd stage) was washed with hydrochloric acid and

leached at solution containing 50 g/L  $\text{Ca}(\text{OCl})_2$  and 100 g/L NaCl for 3 h (S/L=1/5, 25 °C, 600 rpm), to oxidise the remained non-oxidised pyrite particles. This stage was called as 3rd stage. Figs. 2 (c) and 3 (c) with black symbols ( $\blacktriangle$ ) show the changes of the slurry pH and ORP for 3rd stage during leaching, respectively. Initial pH was adjusted 6 to prepare a suitable condition of pH and ORP for dissolution of gold. In this case, changes of pH and ORP were remarked by white symbols ( $\triangle$ ).

Figs. 6 (a)–(c) show the total percent leached gold as a function of time for the three stages of leaching mentioned above. As it is shown, the main gold was extracted at 1st stage of leaching (Fig. 6 (a)). After 3 h leaching, 70.2%, after next 4 h (totally 7 h), 89.3% and after next 3 h (totally 10 h), 93.7% gold was extracted. Since at each stage, ORP of solution is more than 900 mV it can be concluded that the product layer prevents

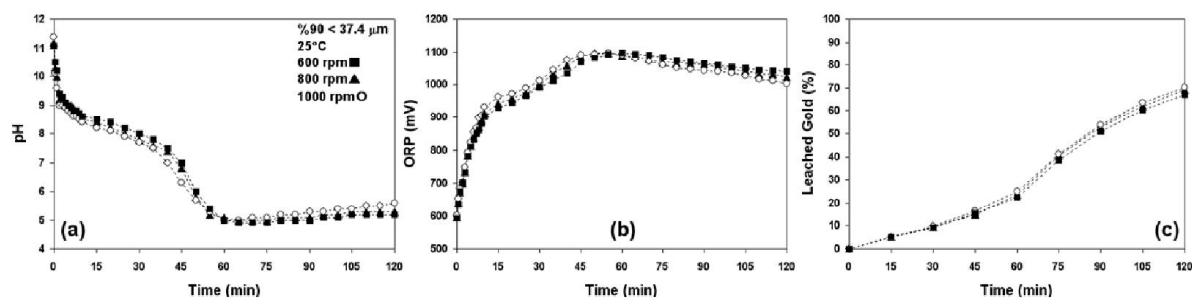


Fig. 7. Effect of stirring speed on (a) pH changes (b) ORP changes (c) percent leached gold.

the progressing of gold leaching at the long time of each stage.

Fig. 6 (a) shows the leaching process of gold at 1st stage includes three steps. At the first 1 h, a moderate increase in the amount of extracted gold is observed. After that, till 2 h, gold recovery increased significantly. Then, the leaching progresses very slowly. Based on Fig. 6 (a), to investigate the effects of stirring speed, temperature and particle size on the dissolution rate and recovery of gold, the time of leaching was selected as 2 h.

### 3. 2. Effect of Stirring Speed

The effect of stirring speed on the leaching of gold was investigated using stirring speeds of 600, 800 and 1000 rpm. Figs. 7 (a) and (b) show the pH and ORP changes of the slurry vs. time for these samples. The results presented in Fig. 7 (c) show that the leaching rate of gold is independent of the stirring speed in the range 600–1000 rpm,

which indicates the reaction is not controlled by the diffusion in the liquid film. Therefore, subsequent experiments were carried out at a stirring speed of 600 rpm.

### 3. 3. Effect of Temperature

Figs. 8 (a) and (b) show the pH and ORP changes of the slurry at various temperatures. At higher temperatures, dropping of pH and rising of ORP are sharper due to increasing in the sulfide oxidation rate. Fig. 8 (c) shows percent recovery of gold vs. time at different temperatures which shows the temperature is more effective on the leaching rate at the first 1 h. At 70 °C hypochlorous acid is consumed quickly and ORP drops to lower than 0.9V, this is a reason for gold precipitation after it is dissolved. At high temperature, it is possible that some of the gangue compounds react with the leachant; thus, the oxidant consumption increases. After 2 h, recovery of gold at 55 °C reached to 69.8% in

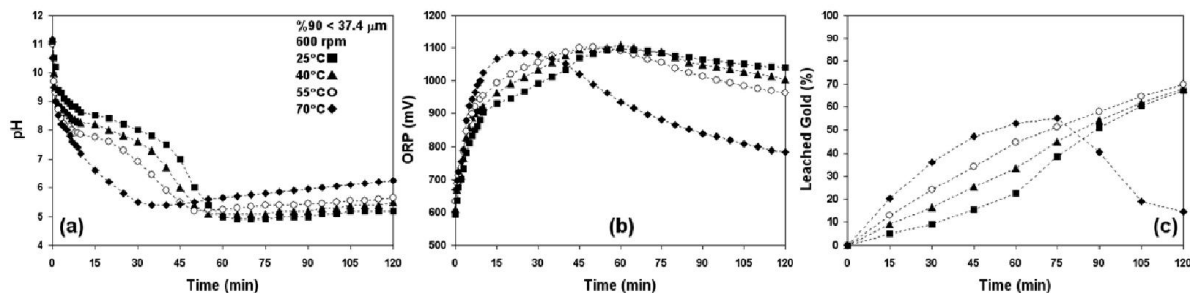


Fig. 8. Effect of temperature on (a) pH changes (b) ORP changes (c) percent leached gold.

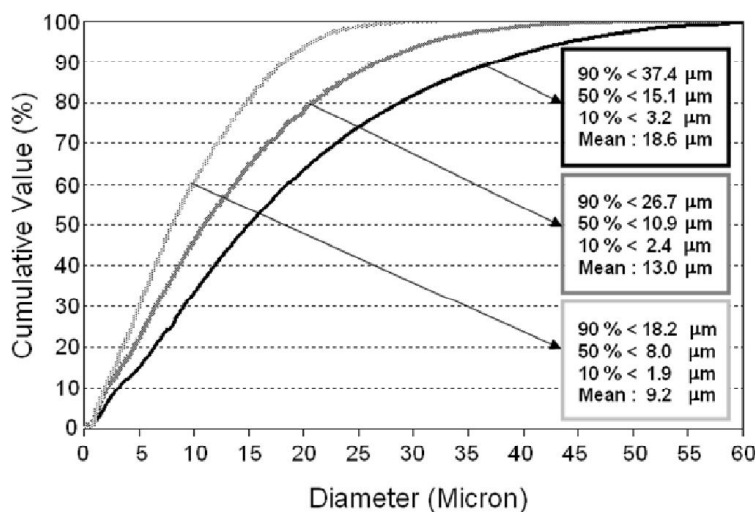


Fig. 9. Particle size distributions of three used concentrates for study of particle size effect.

comparison with 67.1% at 25 °C. In other words, increasing temperature slightly increased the gold recovery.

### 3. 4. Effect of Particle Size

To investigate the effect of particle size on the leaching process, the concentrate was ground by a low energy laboratory ball mill for 2 and 4 h (with concentrate to ball weight ratio: 1/4). Fig. 9 compares particle size distribution of the three concentrates used. By milling for 2 h, particles size decreased from 90% < 37.4 μm to 90% < 26.7 μm and after 4 h, to 90% < 18.2 μm.

Figs. 10 (a) and (b) show the pH and ORP changes of the slurry during leaching for the concentrate with different particle sizes. As the

particle size decreases, pH drops faster. It means that the oxidation of the sulfides is accelerated as the particle size decreases. With faster dropping of pH, ORP is raised faster. Fig. 10 (c) shows faster rate of gold extraction for finer particle size (90% < 18.2 μm). It may be attributed to the higher surface to volume ratio of particles which makes them amenable for more contact with the leachant. After 2 h, percent recovery of gold in the sample with smallest particle size reached to 86.3%.

### 4. DISCUSSION

During leaching of concentrate in chloride–hypochlorite solution, sulfide minerals with pyrite being the main of them are oxidised and

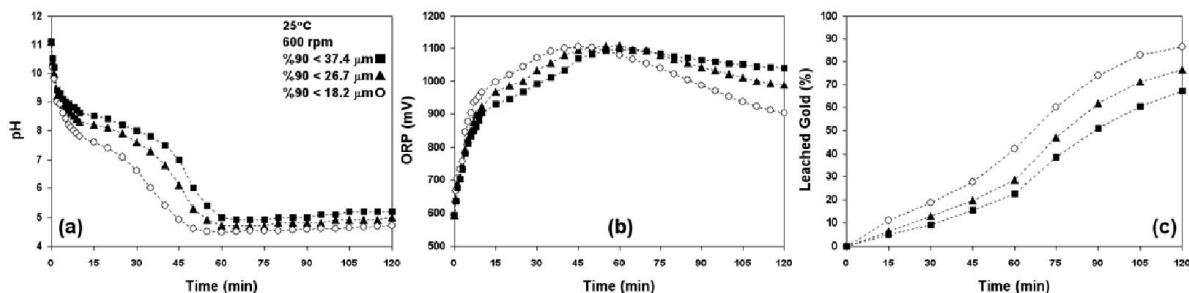


Fig. 10. Effect of particle size on (a) pH changes (b) ORP changes (c) percent leached gold.

acid is produced. Production of acid is the reason for dropping of the slurry pII. At initial pII of 11, hypochlorite ion is the dominant oxidant; whereas, by decreasing pH according to reaction (3) hypochlorous acid (more powerful oxidant) becomes dominant.



Therefore, it is expected that the reaction of gold at the first 1 h is slow; thus, may be chemical reaction controlled. With dropping of pH and formation of hypochlorous acid, reaction rate increased. According to the SEM images, during the leaching reaction an outer layer of an insoluble product was formed and its thickness progressively increased. The oxidant must penetrate through this layer; thus, the leaching rate of gold at the second 1 h might be diffusion controlled.

In hydrometallurgy, the shrinking core model is generally applied to describe the shrinkage of ore particles during mineral leaching reactions. In the shrinking core model, the fraction reacted (X) is related to reaction time (t). When the process is controlled by chemical reaction:

$$\frac{t}{\tau} = 1 - \left(\frac{r_c}{R}\right) = 1 - (1 - X)^{\frac{1}{3}} \quad (4)$$

And if it is controlled by diffusion through product layer:

$$\frac{t}{\tau} = 1 - 3\left(\frac{r_c}{R}\right)^2 + 2\left(\frac{r_c}{R}\right)^3 = 1 - 3(1 - X)^{\frac{2}{3}} + 2(1 - X) \quad (5)$$

Where t is the time required for the particle to react completely,  $r_c$  is the unreacted core radius at a given time (t), R is the initial particle radius. If each of these equations controlled the leaching rate, there must be a linear relation between it and time, which the line slope is called the apparent rate constant (k). The relation between the apparent rate constant and temperature is expressed by equation (6).

$$k = A \exp(-E_a / RT) \quad (6)$$

A is the frequency factor (1/min),  $E_a$  is the

activation energy (J/mol), R is the universal gas constant (8.314 J/mol.K) and T is the reaction temperature (K). By plotting  $\ln(k)$  vs.  $1/T$  and determining the line slope,  $(-E_a/R)$ ,  $E_a$  will be determined. Since a diffusion-controlled process weakly depends on temperature; thus, its activation energy is low [11, 12].

Equations (4) and (5) cannot be applied for the period of the second 1 h since the boundary condition for this section is different; it starts from  $t_1=60$  min rather than  $t_1=0$ . At this condition, equations of chemical controlled (7) and diffusion controlled (8) mechanisms are as below [13]:

$$\frac{t - t_1}{\tau} = 1 - \left(\frac{1 - X}{1 - X_1}\right)^{\frac{1}{3}} \quad (7)$$

$$\frac{t - t_1}{\tau} = 1 - 3\left(\frac{1 - X}{1 - X_1}\right)^{\frac{2}{3}} + 2(1 - (1 - X_1)^{\frac{1}{3}}(X - X_1)) \quad (8)$$

The mentioned equations can be used to describe the leaching process when only one mechanism (chemical reaction or diffusion through the product layer) controls the entire process. Nazemi et al. [14] suggested to share the mechanisms by evaluating the constants of equations (9) and (10), is share of chemical control and is share of diffusion control through product layer.

For first 1 h:

$$t = \tau_1[1 - (1 - X)^{\frac{1}{3}}] + \tau_2[1 - 3(1 - X)^{\frac{2}{3}} + 2(1 - X)] \quad (9)$$

For second 2 h:

$$t - t_1 = \tau_1\left[1 - \left(\frac{1 - X}{1 - X_1}\right)^{\frac{1}{3}}\right] + \tau_2\left[1 - 3\left(\frac{1 - X}{1 - X_1}\right)^{\frac{2}{3}} + 2(1 - (1 - X_1)^{\frac{1}{3}}(X - X_1))\right] \quad (10)$$

Where these constants were calculated by a least square formula as equations (11) and (12):

$$\phi = \sum_i [\tau_1(1 - (1 - X_i)^{\frac{1}{3}}) + \tau_2(1 - 3(1 - X_i)^{\frac{2}{3}} + 2(1 - X_i) - t_i)^2] \quad (11)$$



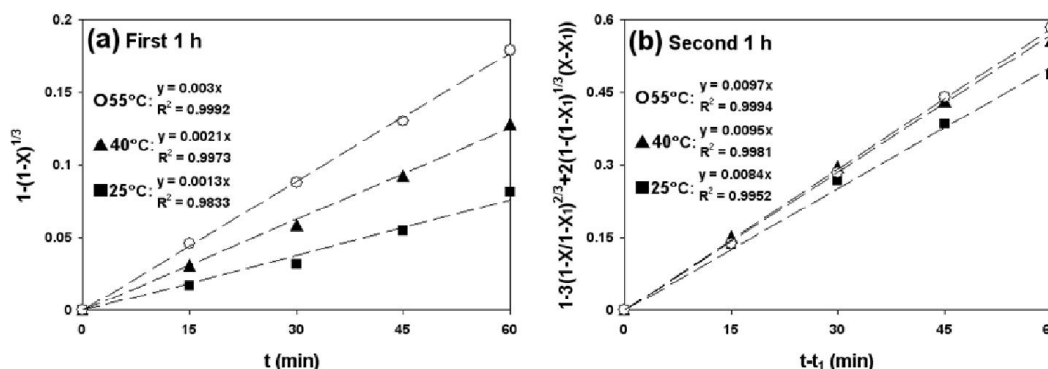


Fig. 11. Plots of (a) chemical control model at first 1 h and (b) diffusion control model at second 1 h of leaching at various temperatures, for calculation of apparent rate constant (k).

Table 2. Data resulted from optimization of Eqs. (11) and (12) for first 1 h and second 1 h of leaching

Parameter			First 1 h			Second 1 h		
			$\tau_1$	$\tau_2$	$R^2$	$\tau_1$	$\tau_2$	$R^2$
600 rpm	25°C	90% < 37.4 $\mu\text{m}$	783.49	0	0.9832	0	119.31	0.9951
800 rpm	25°C	90% < 37.4 $\mu\text{m}$	756.49	0	0.9654	0	109.14	0.9962
1000 rpm	25°C	90% < 37.4 $\mu\text{m}$	710.38	0	0.9671	0	103.27	0.9961
600 rpm	40°C	90% < 37.4 $\mu\text{m}$	479.27	0	0.9972	0	105.21	0.9980
600 rpm	55°C	90% < 37.4 $\mu\text{m}$	338.69	0	0.9991	0	103.18	0.9994
600 rpm	70°C	90% < 37.4 $\mu\text{m}$	135.51	225.17	0.9938	–	–	–
600 rpm	25°C	90% < 26.7 $\mu\text{m}$	600.64	0	0.9883	0	78.10	0.9835
600 rpm	25°C	90% < 18.2 $\mu\text{m}$	388.95	0	0.9710	144.05	0	0.9748

$$\phi = \sum_i [\tau_1 (1 - (\frac{1-X_i}{1-X_1})^{\frac{1}{3}}) + \tau_2 (1 - 3(\frac{1-X_i}{1-X_1})^{\frac{2}{3}} + 2(1 - (1-X_i)^{\frac{1}{3}})(X_i - X_1))] - (t_i - t_1)^2 \quad (12)$$

It must be calculated values of  $\tau$  to obtain minimum value of  $\Phi$ . Calculated results using Microsoft EXCEL have been listed in Table 2. The data of this table indicate that the rate of leaching process at the first 1 h is controlled by chemical reaction and at the second 1 h, the process is diffusion controlled. Increasing the stirring speed had no effect on the controlling mechanism. Increasing the temperature to 55 °C

had no effect but at 70 °C, at the first 1 h controlling mechanism changed to mixed control where the share of diffusion control is more than chemical reaction control and at the second 1 h due to the high consumption of oxidant, ORP dropped to below 900 mV; thus, amount of Au complex in solution was reduced. At second 1 h with reducing the particle size to 90% < 18.2  $\mu\text{m}$ , the controlling mechanism changed from diffusion controlled to chemical reaction controlled, it means that for the fine particles the effect of the product layer is eliminated and due to the high consumption of the oxidant, the reaction rate is reduced.

Figs. 11 (a) and (b) show plots of chemical

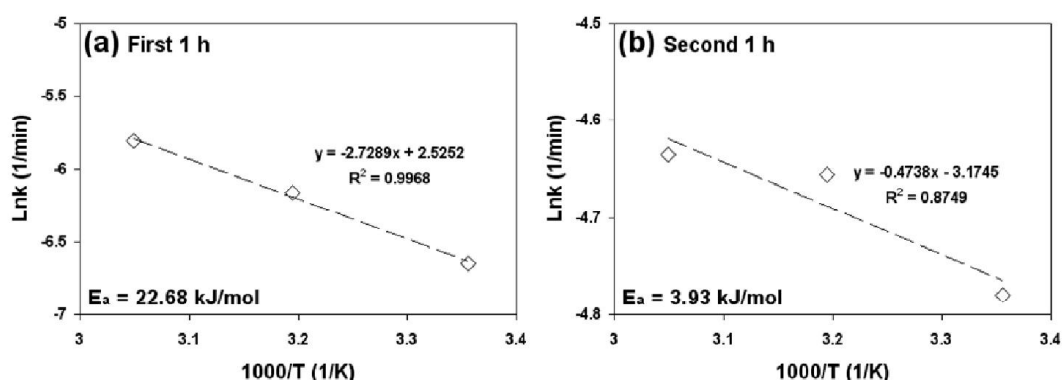


Fig. 12. Plots of  $\ln(k)$  vs.  $1000/T$  for (a) first 1 h and (b) second 1 h of leaching, for calculation of activation energy ( $E_a$ ).

controlled model (Eq. (4)) and diffusion controlled model (Eq. (8)), respectively, using data of gold recovery vs. time. With calculating the slope of these plots (equal to apparent rate constant), activation energy for each mechanism was determined. In Figs. 12 (a) and (b) the plots of  $\ln(k)$  vs.  $1000/T$  are presented for the first 1 h and the second 1 h of leaching, respectively. As it is shown the activation energy for the first 1 h of leaching is 22.68 kJ/mol and for the second 1 h is 3.93 kJ/mol.

## 5. CONCLUSIONS

Chloride–hypochlorite solution was applied for gold leaching of a refractory sulfide concentrate containing 20.45 g/t gold. Leaching tests at different conditions of stirring speed, temperature and particle size were performed. The curves of gold dissolution vs. time showed the role of particle size is more significant than stirring speed and temperature. Experimental data for leaching rate of gold were analyzed with the shrinking–core model. It was concluded that the mechanism of chemical reaction control in the first 1 h of leaching and diffusion control in the second 1 h are prevalent mechanisms which control the leaching rate of gold. Apparent activation energy was calculated 22.68 kJ/mol in the first step and 3.93 kJ/mol in the second step of leaching. In this system in the first step, hypochlorite ion is the dominant oxidant species; therefore, leaching rate of gold is chemically controlled. With decreasing of pH (resulted from

production of acid during oxidation of sulfide) hypochlorite ion is changed to hypochlorous acid which is a stronger oxidant. In the second step, formation of  $\text{Fe}(\text{OH})_3$  as oxidation product of pyrite around the particles (where gold occurs finely disseminated inside them) decreases the leaching rate of gold.

## REFERENCES

1. Ikiz, D., Gulfen, M., Aydın, A. O., “Dissolution kinetics of primary chalcopryrite ore in hypochlorite solution”, *Minerals Engineering*, 19, 972–974.
2. Garlapalli, R. K., Cho, E. H., Yang, R. Y. K., “Leaching of chalcopryrite with sodium hypochlorite”, *Metallurgical and Materials Transactions B*, 41B, 308–317.
3. Jeffrey, M. I., Breuer, P. L., Choo, W. L., “A kinetic study that compares the leaching of gold in the cyanide”, thiosulfate, and chloride systems, *Metallurgical and Materials Transactions B*, 32B, 979–986.
4. Nesbitt, C. C., Milosavljevic, E. B., Hendrix, J. L., “Determination of the mechanism of the chlorination of gold in aqueous solutions”, *Industrial and Engineering Chemistry Research*, 29, 1696–1700.
5. Marsden, J. O., House, C. I., “The chemistry of gold extraction”. 2nd Ed., Society for mining, metallurgy and exploration, Colorado, USA, pp. 185–190.
6. Puvvada, G. V. K., Murthy, D. S. R., “Selective precious metals leaching from a chalcopryrite

- concentrate using chloride/hypochlorite media”  
, *Hydrometallurgy* ,58, 185–191.
7. Baghalha, M., “Leaching of an oxide gold ore with chloride/hypochlorite solutions”, *International Journal of Mineral Processing*, 82, 178–186.
  8. Soo Nam, K., Hi Jung, B., Woong An, J., Jun Ha, T., Tran, T., Jun Kim, M., “Use of chloride–hypochlorite leachants to recover gold from tailing”, *International Journal of Mineral Processing*, 86, 131–140.
  9. Ghobeiti Hasab, M., Rashchi, F., Raygan, Sh., “chloride–hypochlorite oxidation and leaching of refractory sulfide gold concentrate”, *Physicochemical Problems of Mineral Processing*, 49 (1), 61–70.
  10. Perez–Lopez, R., Cama, J., Nieto, J. M., Ayora, C., “The iron–coating role on the oxidation kinetics of a pyritic sludge doped with fly ash”, *Geochimica et Cosmochimica Acta*, 71, 1921–1934.
  11. Habashi, F., “Kinetics of Metallurgical Processes”, Second Edition, Metallurgie Extractive Quebec, Canada.
  12. Levenspiel, O., “Chemical Reaction Engineering”, Second Edition, Wiley, New York.
  13. Aarabi–Karasgani, M., Rashchi, F, Mostoufi, N., Vahidi, E., “Leaching of vanadium from LD converter slag using sulfuric acid”, *Hydrometallurgy*, 102, 14–21.
  14. Nazemi, M. K., Rashchi, F., Mostoufi, N., “A new approach for identifying the rate controlling step applied to the leaching of nickel from spent catalyst”, *International Journal of Mineral processing*, 100, 21–26.